Preprints of the 19th World Congress
The International Federation of Automatic Control
Cape Town, South Africa. August 24-29, 2014

A Wavelet-based Approach to Improve Foggy Image Clarity

Jianfang Jia*, Hong Yue**

** North University of China, Taiyuan 030051, China*
(e-mail: jiajf2002@163.com).
*** Department of Electronic and Electrical Engineering, University of Strathclyde, Glasgow G1 1XW, UK*
(e-mail: hong.yue@strath.ac.uk)

Abstract: Under foggy viewing conditions, image contrast is often significantly degraded by atmospheric aerosols, which makes it difficult to quickly detect and track moving objects in intelligent transportation systems (ITS). A foggy image visibility enhancing algorithm based on an imaging model and wavelet transform technique is proposed in this paper. An optical imaging model in foggy weather conditions is established to determine the image degradation factors and compensation strategies. Based on this, the original image is firstly transferred into YUV color space of a luminance and two chrominance components. Then the luminance component is decomposed through wavelet transform into low- and high-frequency subbands. In the low-frequency subband, the medium scattered light component is estimated using Gaussian blur and removed from the image. Nonlinear transform for enhancement of foggy images is applied to high-frequency subbands. In the end, a new image is recovered by combining the chrominance components and the corrected luminance component altogether. Experimental results demonstrate that this algorithm can handle the problem of image blurring caused by atmospheric scattering effectively, and has a better real-time performance compared with a standard model-based procedure.

Keywords: Image processing, optical image modeling, wavelet transform, visibility, image restoration, fog removal, intelligent transportation system (ITS).

1. INTRODUCTION

Image processing plays an important role in intelligent transportation systems (ITS), and has extensive applications in traffic control and traffic safety monitoring (Masaki, 1998; Cucchiara et al, 2000; Atev et al., 2005). It is always a difficult task to obtain high quality images of outdoor moving objects under poor weather conditions such as a heavy fog. Images captured in a foggy environment normally have low level of contrast and resolution, which largely decreases image details and reduces level of recognition. This is because lots of aerosol in air causes attenuation and scattering of light in the path from the scene to the spread of the camera, which is directly related to the size and the number of suspended particles in the air. The larger the size and number of the suspended particles is, the more serious effect it has on light reaching the camera. Scattering is regarded as the main reason for reducing quality of images. It not only reduces the transmission of light energy, but also causes changes in the direction of light. Attenuation only weakens the intensity of light, and has relatively smaller influence on imaging. Therefore, the tasks of foggy image processing include removing atmospheric scattering effect, enhancing image details, and complete reconstruction of images.

In recent years, there has been considerable research in image processing under foggy weather (Oakley and Satherley, 1998, Hautiére and Aubert, 2005; Hautiére et al, 2006; Hiramastu et al 2008; Desai et al, 2009). There are two main groups of methods on foggy image processing: the non-model methods and the enhancement algorithms based on imaging models. The non-model image sharpness algorithms can effectively improve the contrast level of foggy images, highlight image details and enhance the image visibility (Hassan and Aakamatsu, 2006; Tarel et al, 2010). These methods improve image quality mainly by image enhancement. The specific causes that reduce image quality are not identified. This inevitably results in loss of image information and distortion of processed images. In addition, the non-model algorithms cannot guarantee the consistency of adjacent video frame images after processing.

In model-based algorithms, the physical process that produces a fog-degraded image is investigated, and a degradation model of the foggy image is established. The invert image contrast reduction process is obtained, thus the distortion caused by the degradation process is compensated that can achieve the optimal estimate of a defogging image, and recover a high-quality image. A method of extracting the scene depth information was proposed to restore scene contrast using supplementary information of an image, such as wavelength of the environmental light, color depth information, etc (Narasimhan and Nayar, 2003; Schechner and Nayar, 2005). An automatic haze removal algorithm was proposed in (Guo et al, 2011), in which a multi-scale Retinex algorithm was used on the luminance component. He et al (2011) proposed a method to remove haze from a single image based on the so-called dark channel prior, which is regarded as statistics of outdoor haze-free images. They

argued that most local patches in outdoor haze-free images contain pixels whose intensity is very low in at least one color channel. Applying this assumption with the haze imaging model, the thickness of the haze can be directly estimated and a high-quality haze-free image can be recovered under certain conditions.

It is believed that there will be less loss of image information and can better improve the quality of foggy images using model-based model sharpness algorithms. However, these methods still have drawbacks in practice. Firstly, they normally require a large amount of image processing time to estimate the medium scattered light or the depth of field information. Secondly, the invert process of image degradation possibly exists during the process of image processing, but this is often unknown. In addition, image degradation is also subject to interference and noise, which bring disturbances and uncertainties to recovery of foggy images. To achieve a better image restoration from a foggy environment, it is necessary to analyze accurately the causes for the degradation of image quality, understand its inverse process, and establish a reliable foggy image degradation model. This motivates our work in this paper.

The remainder of this paper is organized as follows. In Section 2, an optical imaging model of foggy images is developed in detail. The primary steps of the foggy image visibility enhancement algorithm are given in Sections 3. The experimental results are presented in Section 4. Finally, the main conclusions are summarized in Section 5.

2. OPTICAL IMAGING MODEL OF FOGGY WEATHER

Fig. 1 shows the optical path associated with a camera sensor when there are suspended particles in air.

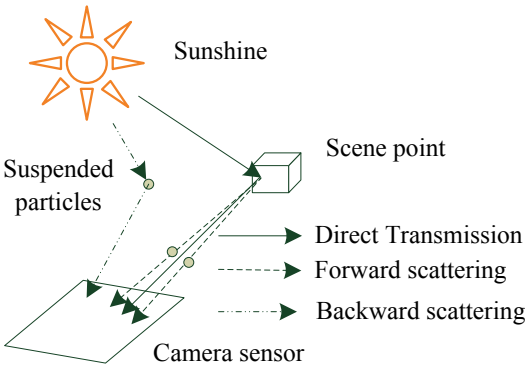

Fig. 1. The optical imaging model in foggy weather

The optical imaging model describes the way light gets attenuated as it traverses from a scene point to the sensor. The imaging quality is affected by the presence of suspended particles in foggy weather. Due to atmospheric scattering, a fraction of light flux is removed from the incident beam. The unscattered flux, called direct transmission, is transmitted to the sensor. Thus, the foggy image can be regarded as the linear superposition of three parts: direct transmission E_d, forward scattering E_f, and backward scattering E_b. Referring to Fig. 1, E_b has an large effect on imaging process - it adds a layer of fuzzy fog curtain to a foggy image. E_f is transmitted to the sensor from the scene point through suspended particles, which blurs the foggy image. These two parts cause image quality degradation and lead to poor brightness, blurring edge, and low contrast in produced images. Since E_b and E_f are difficult to be distinguished between each other from the surrounding environment, they are together referred to as medium scattered light E_{fb}, which is described as

$$E_{fb}(x) = E_\infty \left(1 - \mathrm{e}^{-\beta d(x)}\right) \tag{1}$$

where E_∞ is the atmospheric light, $d(x)$ is the scene depth at pixel position x, and β denotes the attenuation coefficient of the atmosphere. E_d, the irradiance at the sensor due to reflected light, is given by

$$E_d(x) = E_\infty \rho(x) \mathrm{e}^{-\beta d(x)} \tag{2}$$

where a function $\rho(x)$ is the reflectance of the object observed and describes the reflectance properties of the scene point and the spectral reflectance effect of the camera sensor.

The total irradiance received by a camera sensor is the sum of E_d and E_{fb}. Thus, the imaging model in foggy conditions can be expressed as

$$\begin{aligned} E_T(x) &= E_d(x) + E_{fb}(x) \\ &= E_\infty \rho(x) \mathrm{e}^{-\beta d(x)} + E_\infty (1 - \mathrm{e}^{-\beta d(x)}) \end{aligned} \tag{3}$$

where $E_T(x)$ represents the apparent luminance at pixel position x. This model can be directly extended to a color image by applying the same model to each RGB component.

According to (1) and (2), E_{fb} is strengthened exponentially with the increase of the depth of field distance, while E_d damps exponentially with the increase of the depth of field distance. Therefore, the main causes of foggy image blurring and low contrast are attenuation and scattering. Restoration of foggy images is the process of restoring $E_\infty \rho(x)$ based on the imaging model (3). It can be derived from (3) that

$$E_\infty \rho(x) = (E_T(x) - E_{fb}(x)) \mathrm{e}^{+\beta d(x)} \tag{4}$$

As a result, the key factors of recovering the foggy image are to accurately estimate the medium scattering factor E_{fb} and the depth of field information $\mathrm{e}^{+\beta d(x)}$.

3. A FOGGY IMAGE ENHANCEMENT ALGORITHM

3.1 Image Enhancement Algorithm with Wavelet Transform

For imaging of moving objects in ITS, the distance range of interest is relatively short, normally not more than a few hundred meters. It is therefore assumed that there is no spatial change in the properties of foggy weather and homogeneous atmosphere is considered. Under this assumption, the following algorithm is proposed to enhance foggy image clarity based on the optical imaging model in Section 2. The

main idea is to remove the medium scattered light effect and enhance the contribution from direct incident light. The flowchart of the algorithm is illustrated in Fig. 2.

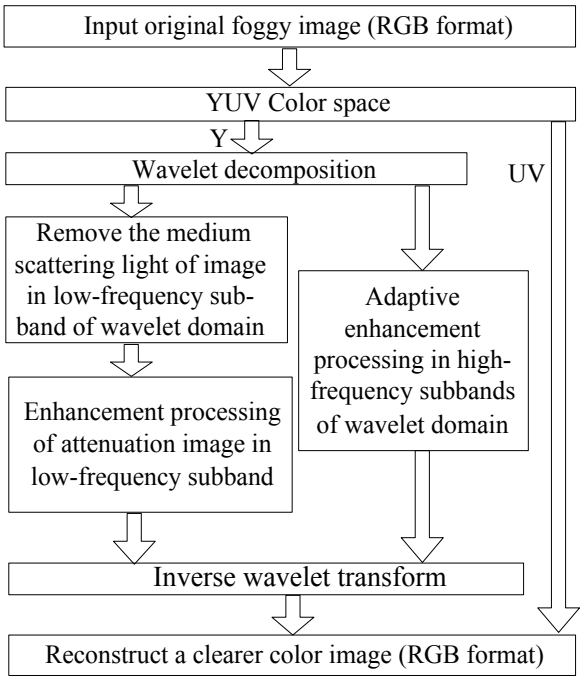

Fig. 2. Flowchart of the foggy image processing algorithm

The algorithm consists of four major steps explained as follows.

Step 1. Color space transformation and wavelet transform. The original foggy image in RGB (Red-Green-Blue) color format is transformed to the YUV color space that comprises of a luminance component (Y) and two chrominance components (U, V). Apply wavelet decomposition to the luminance component Y to get a low-frequency subband, LL_n, and multiple high-frequency subbands LH_i, HL_i, HH_i ($i = 1, 2, \cdots, n$), where n is the order of wavelet decomposition. Here LL, LH, HL and HH stands for low-low, low-high, high-low and high-high subbands, respectively.

Step 2. In the low-frequency subband of wavelet domain, the medium scattered light component of a foggy image is estimated and removed. Then, the image is enhanced adaptively via employing the corrected attenuation factor following the local complexity.

Step 3. In the high-frequency subbands of wavelet domain, adaptive enhancement of a foggy image is conducted.

Step 4. Inverse wavelet transform and image color space conversion. Apply inverse wavelet transform to the enhanced wavelet coefficients and obtain the enhanced luminance component Y'. Y' and UV components are reconstructed to form a clearer YUV image, and this YUV image is converted back to an RGB colored image.

In this algorithm, the image transform to YUV space separates the luminance component, *Y,* from the chrominance components. The wavelet transform decomposes *Y* further into a low-frequency subband and several high-frequency subbands. Image processing is then conducted to low- and high-frequency subbands separately.

3.2 Image Enhancement Processing in Low-Frequency Subband

The medium scattered light component lies mainly in the low-frequency domain of a foggy image. Using the optical imaging model, this component can be estimated through the Gaussian blur method and then removed directly from the original image. The remaining image information is from the attenuated direct incident light. Enhancing the attenuated information will recover the low-frequency sub-image.

Images of moving vehicles in foggy weather conditions are normally taken within a short distance, therefore the attenuation information is enhanced by means of an nonlinear adjustment based on local complexity. The following steps are implemented in the low-frequency sub-band processing.

Step 1. In the low-frequency subband of wavelet domain, LL_n, the Gaussian smoothing image G_n is obtained by Gaussian blur, which is taken as an estimation of the medium scattered light information E_{fb}. This estimated G_n is then removed from LL_n to get Y_1.

Step 2. Since the values of Y_1 are relatively small and some are negative, a correction value of Y_δ is added to Y_1 so as to be match the overall brightness of LL_n. The value of Y_δ is determined by

$$Y_\delta = \overline{LL_n} - \overline{Y_1} \tag{5}$$

where $\overline{LL_n}$ and $\overline{Y_1}$ are the mean values of LL_n and Y_1, respectively. The corrected low-frequency sub-band information forms the direct incident light attenuation part:

$$Y_2 = Y_1 + Y_\delta \tag{6}$$

Step 3. Y_2 is then multiplied by the attenuation factor $e^{+\beta d(x)}$ to recover the low-frequency sub-graph Y_3, i.e.,

$$Y_3 = Y_2 e^{+\beta d(x)} \tag{7}$$

Using (1), the attenuation factor $e^{+\beta d(x)}$ can be calculated by

$$e^{+\beta d(x)} = \frac{E_\infty}{E_\infty - E_{fb}} \approx \frac{\{Y_{LL_n}\}_{\max}}{\{Y_{LL_n}\}_{\max} - G_n} \tag{8}$$

$\{Y_{LL_n}\}_{\max}$ is the maximum coefficient of subband Y_{LL_n}. Following the work in (Tan, 2008), the atmospheric light, E_∞, can be obtained from pixels that have the highest intensity in the input image. Hence, $\{Y_{LL_n}\}_{\max}$ is used as the estimated value of E_∞. It should be noted that $e^{+\beta d(x)}$ is a function of pixel position (i, j) through $x(i, j)$ and $G_n(i, j)$.

Step 4. The attenuation factor $e^{+\beta d(x)}$ is further corrected by a nonlinear adjustment based on local complexity. For a local

image region defined by $N=(2n+1)\times(2n+1)$ pixels, its complexity, $C_P(i,j)$, satisfies $1 \le C_P(i,j) \le N$, where (i, j) represents the position of an image pixel. A large $C_P(i,j)$ corresponds to a large variation of luminance in this local region, where the attenuation factor should have a larger value than that of a darker and less changing area.

Using $\lambda(i, j)= e^{+\beta d(x)}$ to stand for the attenuation factor at each pixel position (i, j), the corrected attenuation factor in the defined local region is calculated by

$$\lambda'(i,j) = \bar{\lambda} + (C_P(i,j) - (N+1)/2) \times \Delta d \quad (9)$$

where $\bar{\lambda}$ is the averaged value of $\lambda(i,j)$. Δd is the scale adjustment coefficient, whose value is normally set to 0.1. Using this corrected attenuation factor, the low-frequency sub-band coefficient $Y_3^{'}$ is

$$Y_3^{'} = Y_2 \times \lambda^{'}(i,j) \quad (10)$$

3.3 Image Enhancement Processing in High-Frequency Subbands

A high-pass filter is designed to enhance the image information in high-frequency subbands. The enhancement coefficient for high-frequency subbands is calculated by the modified Butterworth filter

$$H(j,\omega_h,\omega_v) = r_1 - \frac{r_2}{1+2.415\times\left[\sqrt{\omega_h^2+\omega_v^2}\Big/\left(2^j\times k_c\right)\right]^{2^n}} \quad (11)$$

where ω_h and ω_v are the horizontal and vertical weighting coefficients, respectively. For wavelet decomposition subband LH_j, $\omega_h = 0, \omega_v = 1$; for HL_j, $\omega_h = 1, \omega_v = 0$; for HH_j, $\omega_h = 1, \omega_v = 1$. The parameter j is the wavelet decomposition progression $(j = 1, 2\cdots n)$, and 2^j is the corresponding resolution. r_1 and r_2 are called the modification factors, and k_c is the cut-off coefficient. The best setting of these parameters are determined by trial-and-error in image processing.

Using the high-pass filter in (11), it is necessary to apply nonlinear transform to coefficients of high-frequency subbands so as to enhance high-frequency information and suppress noise terms. The following adaptive enhancement algorithm is applied:

$$\omega_{out} = \begin{cases} 0, & -T \le \omega_{in} \le T \\ H(j,\omega_h,\omega_v)\times\omega_{in}, & otherwise \end{cases} \quad (12)$$

where T denotes the threshold value, and $T = \sigma_1\sqrt{2\log(m)/m}$ (Donoho, 1994). σ_1 is the mean square deviation of high-frequency coefficients; m is the number of high-frequency subband coefficients of LH_j, HL_j, HH_j. ω_{in} and ω_{out} are the coefficients before and after wavelet transformation, respectively. Within the range of $[-T, T]$, ω_{out} is set to zero to suppress the image noise, and in all other ranges the image details are enhanced by coefficient H.

4. EXPERIMENTAL RESULTS AND ANALYSIS

The proposed algorithm is tested in processing images of city roads under different foggy weather conditions. Two images are used in the simulation study; one is taken under a light fog, the other taken under a heavier fog and has less visibility. The original images are in standard JPEG format. Both visual check by human eyes and a quantitative measure of the contrast level of an image are used to evaluate the quality of enhanced images. In general, if an image has a better clarity, its contrast level is also higher, which indicates a high image quality. The image contrast coefficient C can be expressed by (Annadurai and Shanmugalakshmi, 2007)

$$C = \sum_{\Delta} \Delta(i,j) P(i,j) \quad (13)$$

where $\Delta(i,j) = |i-j|$ is the absolute value of grey level difference between pixels, $P(i,j)$ is the discrete probability distribution function of grey level at each pixel. Adjacent pixels can be four- neighborhood-pixels or eight-neighborhood-pixels. Four-neighbor-pixels region is used to calculate the value of C in this work.

The proposed algorithm is compared with a standard model-based image enhancement method. The same imaging model is used for both algorithms, and the image processing operations are all conducted in the YUV color space. However, in the standard method, the luminance component Y is not decomposed with wavelet transform, therefore the full Y is processed rather than the low-frequency subband in the proposed algorithm. The Gaussian smoothing image G_n is estimated through Gaussian convolution to remove the blur image caused by the medium scattered light. Then G_n is substituted into (8) to compute the attenuation factor $e^{+\beta d(x)}$, which are taken into (7) to obtain the recovery luminance component Y_3. The YUV image is composited using the UV components of the original image together with the compensated Y_3. Finally, the enhanced RGB image is obtained through color space conversion.

Using the proposed algorithm, the luminance component Y is decomposed with a third-order wavelet transform (n=3). In the low-frequency subband LL_3, the coefficient $Y_3^{'}$ is obtained from convolution of a small scale parameter and a small image template. The size of the Gaussian template is 11 by 11, and the Gaussian radius σ is set to be 2. In fact, when only the low-frequency subband is considered, the Gaussian smoothing can achieve a better smoothing effect than handling the full Y. In high-frequency subbands, the modification factors and the cut-off coefficient of high-pass filter are set to be $r_1 = 2.8$, $r_2 = 2.0$, and $k_c = 0.5$, respectively.

For the first image, the processing results using the standard model-based method and the proposed algorithm are shown in Fig.3.

(3a) Original foggy image

(3b) Image processed by a traditional model-based method

(3c) Enhanced image from the proposed method

Fig. 3. Image processing: light fog weather.

The image contrast coefficient C is computed using (13) for the three images in Fig.3 with values being 17.519, 30.581, and 44.800, respectively. The fog obviously affects the image visibility. The original image is blur and has a low contrast level. It can be seen from Fig. (3c) that the image processed with the proposed algorithm contains richer image details, and its image contrast C is the highest among the three images, which means the enhanced image keeps natural color and contrast with a better quality.

The image processing results for a heavier fog situation are illustrated in Fig.4. Fig. (4a) is the original traffic image, and its contrast value of C is 9.379, which is much lower than that of Fig. (3a) under a light fog. The value of C for the image in Fig. (4c) is 33.028, and it is higher than that of Fig. (4b) handled by the standard model-based method, which is 30.271 for Fig. (4b). Again, the proposed algorithm demonstrates a better quality in processing foggy images.

(4a) Original foggy image

(4b) Image processed by a traditional model-based method

(4c) Enhanced image from the proposed method

Fig. 4. Image processing: heavier fog weather.

When the medium scattered light is estimated using the proposed algorithm, Gaussian smoothing is performed in the low-frequency subband LL_3 of the Y component. The size of Gaussian template is only 1/64 of the original image size. In contrast, the standard method estimates the luminance component of the original image using Gaussian convolution directly from the medium scattered light, and its smoothing operation is carried out on the whole image. To achieve

similar results obtained by the proposed algorithm, the size of the Gaussian template for the standard method needs to be 41 by 41, and the Gauss radius σ is set to be 16. It can be seen a much larger template is used and this consumes more computational efforts in processing the same image.

The image processing time of 3 images of different sizes using the two methods are compared in Table 1. A PC with Pentium CPU 2.16 GHz and 1GB memory is used; and the software is Microsoft Visual C++ 6.0. It can be seen from Table 1 that the processing time using the proposed algorithm is significantly less than that of the standard model-based method. This means the proposed algorithm has a better real-time performance, and has a good potential to be applied to processing of real-time videos in ITS.

Table 1. Image processing time of the traditional model-based method and the proposed algorithm

Image size (pixel)	Image processing time (ms)	
	the traditional model-based method	the proposed algorithm
320×240	2, 266	32
480×320	4, 594	47
720×576	12, 578	125

5. CONCLUSIONS

In this paper, we present a new method to improve the clarity of foggy images using an optical imaging model and wavelet decomposition technique. The original RGB image is converted to a YUV color space, and the luminance component *Y* is processed with wavelet decomposition into a low-frequency subband and a number of high-frequency subbands. Thus, the problems of image blur and uneven illumination are handled in the low-frequency subband only, and a high-pass filter is designed to enhance the image details in high-frequency subbands. A much clearer foggy image is achieved by means of the proposed algorithm. Compared with a standard model-based method without using wavelet decomposition, the proposed algorithm can effectively improve the foggy image clarity, and significantly reduce the image processing time, therefore provides a fast defogging method to restore images affected by different densities of fog in real-time applications.

This algorithm is mainly useful for outdoor applications when the foggy images are captured from a short distance of the scene point. It is still difficult to defog heavily foggy images taken from a far distance of the scene. This is because information for image restoration is insufficient under this situation. For the same reason, the proposed algorithm could be inadequate when applied to nocturnal conditions. Further investigation is underway to tackle these problems.

ACKNOWLEGEMENT

This work is partly supported by the National Natural Science Foundation of China (51375462). The authors would like to thank Miss Xiangfeng Guo for help with simulation.

REFERENCES

Annadurai, S., Shanmugalakshmi, R. (2007). *Fundamentals of Digital Image Processing*. Pearson Education, India.

Atev, S., Arumugam, H., Masoud, O., Janardan, R., and Papanikolopoulos, N.P. (2005). A vision-based approach to collision prediction at traffic intersections. *IEEE Trans. Intell. Transp. Syst.*, 6(4), 416-423.

Cucchiara, R., Piccardi, M., and Mello, P. (2000). Image analysis and rule-based reasoning for a traffic monitoring system. *IEEE Trans. Intell. Transp. Syst.*, 1(2), 119-130.

Desai, N., Chatterjee, A., Mishra, S., Chudasama, D., Choudhary, S., and Barai, S.K. (2009). A fuzzy logic based approach to de-weather fog-degraded images. In *Proc. 6th Int. Conf. Computer Graphics, Imaging and Visualization*, 383-387.

Donoho, D.L and Johnstone, I.M. (1994). Ideal spatial adaptation via wavelet shrinkage. *Biometrika*, 81, 425-455.

Guo, F., Cai, Z.X., and Xie, B., and Tang, J. (2011). New algorithm of automatic haze removal for single image. *Journal of Image and Graphics*, 16(4), 516-521.

Hassan, N.Y., Aakamatsu, N. (2006). Contrast enhancement technique of dark blurred image. *Int. J. Computer Science and Network Security*, 6(2A), 223-226.

Hautiére, N., Aubert, D. (2005). Contrast restoration of foggy images through use of an onboard camera. In *Proc. 8th Int. Conf. Intell. Transp. Syst.*, 601-606.

Hautiére, N., Tarel, J.P., and Lavenant, J., and Aubert, D. (2006). Automatic fog detection and estimation of visibility distance through use of an onboard camera. *Machine Vision and Applications*, 17(1), 8-20.

He, K.M., Sun, J., and Tang, X.O. (2011). Single image haze removal using dark channel prior. *IEEE Trans. Pattern Anal. Mach. Intell.*, 33(12), 2341-2353.

Hiramatsu, T., Ogawa, T., and Haseyama, M. (2008). A Kalman filter based restoration method for in-vehicle camera images in foggy conditions. In *Proc. Int. Conf. Acoustics, Speech and Signal Processing*, 1245-1248.

Masaki, I. (1998). Machine-vision systems for intelligent transportation systems. *IEEE Intelligent Systems and their Applications*, 13(6), 24-31.

Narasimhan, S.G., Nayar, S.K. (2003). Contrast restoration of weather degraded images. *IEEE Trans. Pattern Anal. Mach. Intell.*, 25(6), 713-724.

Oakley, J.P. and Satherley, B.L. (1998). Improving image quality in poor visibility conditions using a physical model for contrast degradation. *IEEE Trans. Image Process.*, 7(2), 167-179.

Schechner, Y.Y. and Nayar, S.K. (2005). Generalized mosaicing: polarization panorama. *IEEE transactions on pattern analysis and machine intelligence*, 27(4), 631-636.

Tan, R.T. (2008). Visibility in bad weather from a single image. in *IEEE Conf. Computer Vision and Pattern Recognition*, 1-8.

Tarel, J.P., Hautière, N., Cord, A., Gruyer, D., and Halmaoui, H. (2010). Improved visibility of road scene images under heterogeneous fog. In *Proc. 2010 IEEE Intelligent Vehicles Symp.*, 478-485.